Title
THE MICROSTRUCTURE AND PROPERTIES OF MARTENSITE FORMED FROM CYCLICALLY TRANSFORMED AUSTENITE

Author
Ravi, K.V.

Publication Date
1965-08-01

UCRL-16121

University of California

Ernest O. Lawrence Radiation Laboratory

THE MICROSTRUCTURE AND PROPERTIES OF MARTENSITE FORMED FROM CYCLICALLY TRANSFORMED AUSTENITE

Berkeley, California

DISCLAIMER

UNIVERSITY OF CALIFORNIA
Lawrence Radiation Laboratory
Berkeley, California

AEC Contract No. W-7405-eng-48

THE MICROSTRUCTURE AND PROPERTIES OF MARTENSITE FORMED FROM CYCLICALLY TRANSFORMED AUSTENITE

K. V. Ravi
(M.S. Thesis)

August 1965

THE MICROSTRUCTURE AND PROPERTIES OF MARTENSITE FORMED FROM CYCLICALLY TRANSFORMED AUSTENITE

Contents

THE MICROSTRUCTURE AND PROPERTIES OF MARTENSITE FORMED FROM CYCLICALLY TRANSFORMED AUSTENITE

K. V. Ravi

Inorganic Materials Research Division,
Lawrence Radiation Laboratory,
Department of Mineral Technology, College of Engineering,
University of California, Berkeley, California

ABSTRACT

By the employment of solid state transformation and thermo-mechanical treatments on steel, microstructures with enhanced mechanical properties have been produced.

A thermo-mechanical treatment comprising of deforming the steels in the austenitic condition followed by a cyclic heat treatment of alternate heating to an elevated tempering temperature and cooling to progressively decreasing cryogenic temperatures was employed.

Metallography, hardness measurements and mechanical testing were utilized to evaluate the results of the process.

The steels optimally processed had microstructures of either an essentially martensitic matrix (the high carbon steels) or a composite austenitic martensitic material that was predominately austenitic (the low carbon steel).

The low carbon steel exhibited yield strengths in excess of 200,000 psi with elongation of 28 percent. Austenite instability was noted in the stress-strain curves of the high carbon steel and was not evident in the lower carbon steel.

I. INTRODUCTION

A broad definition of a high strength steel is the simple criterion that the steel has a yield strength of 200,000 psi or higher with adequate ductility.[1] Combined with this is the requirement of a minimum of ten percent elongation for structural parts that are highly stressed.

For satisfactory service cracks initiated in a highly stressed material should not propagate and lead to failure. This requires that stress concentrations be redistributed by means of local plastic flow. This is achieved by providing conditions such that dislocations in the material can move across the locally stressed regions thereby affording stress relief. However such a property is in direct conflict with the requirement that dislocation motion be impeded in high strength materials.

Strength in materials is achieved by blocking the motion of dislocations within the crystal. It has been shown[2] that dislocations in plastically deformed metals tend to collect in tangled networks with the portions inside the network being free of dislocations. The tangled regions act as obstacles to the motion of other dislocations generated during subsequent plastic deformation thus increasing the stress required to cause further plastic flow. By cold work the distance between obstacles can be decreased. However it has been found that the minimum distance achieved in this manner is about 0.5 microns.[2] Thus there is an upper limit to the strength that can be obtained by cold working alone.

From the relationship* $\tau_y = \frac{Gb}{\ell}$, or $\sigma_y = \frac{2Gb}{\ell}$ for the tensile yield it is necessary to have barriers only 15 to 25 atom distances apart to furnish the theoretical tensile yield strength of a material. However such a material would not have any ductility since dislocations cannot move. It is hence necessary for the barriers to be at a greater distance apart than the minimum theoretical distance.[3]

The microstructural requirement for high strength therefore would be one having a fine dispersion of a hard second phase with optimum spacing for strength and ductility.

The strongest steels currently available are those that have been ausformed. Ausforming is the process by which steel is deformed in the austenitic condition and the deformed austenite subsequently transformed to martensite.[4] This process of strengthening has been the subject of numerous investigations which have been recently reviewed in a paper by Phillips and Duckworth.[5] Deformation is an important parameter in this process. Plastic deformation of austenite is thought to induce a number of microstructural changes. The most obvious change is the increase in dislocation density. Closely spaced nucleation sites are created on which carbides can form and also it is thought that plastic deformation has the effect of accelerating the diffusion of substitutional elements. Thus, these processes are presumed to lead to the nucleation of alloy carbides during deformation of the austenite, as proposed by various authors.[6-10] The alloy carbides act as obstacles

---

* τ_y = shear yield stress, σ_y = tensile yield stress, G = the shear modulus, b = the Burgers vector, and ℓ = the distance between precipitate particles which are not cut by dislocations.

to dislocation motion in the same way as dislocation networks or tangles do. A dispersed phase resists dislocation motion by pinning of dislocations until the applied stress overcomes the pinning by breaking the barriers or by the cross-slip of dislocations around the particles.

The ausform process requires that the austenite be deformed in the "bay" region of the transformation diagram. This region is usually stable at a high temperature and this fact limits the flexibility of the process.

The present work is an attempt to develop a more flexible thermo-mechanical process, making use of known theories and processes, for the development of high strength and ductility in steels.

Suitably designed alloy steels were austenitized at temperatures where complete carbide solubility was obtained. The austenite was deformed at different temperatures. Following deformation the austenite is quenched to a temperature just below the M_s temperature, then re-heated to an intermediate temperature (cycle tempering temperature) to temper the martensite that is formed, followed by quenching to a lower temperature to form more martensite which is again tempered as before at the cycle tempering temperature. The process is repeated by quenching to successively lower temperatures with intermediate tempering. The lowest quenching temperature was that of liquid nitrogen.

The investigation includes studies of the effect of chemical composition and thermo-mechanical variables on microstructure and mechanical properties at the different stages of the processes involved.

II. EXPERIMENTAL PROCEDURE

A. Alloy Composition

The two main requirements to be met in the design of the alloy are (a) and M_s temperature well below room temperature (about -35°C) so that the austenite is stable at room temperature and (b) a balance is maintained between the carbide formers and carbon in the steel.

In balancing the carbon content against carbide formers sufficient chromium and molybdenum was added to combine with all the carbon in the alloy. Three chromium carbides are reported to be present[11] ($Cr_{23}C_6$, Cr_7C_3 and Cr_3C_2). Extraction replica work has shown that the precipitates found in the greatest abundance in alloy steels with Cr are $Cr_{23}C_6$.[9] In the case of molybdenum, MoC and Mo_2C are reported,[11] however it has been shown that the precipitates in ausformed alloys are MoC.[12] The alloys were designed by making the assumption that Cr forms $Cr_{23}C_6$ and Mo forms MoC. The nickel was added to balance the M_s of the alloy.

Silicon was added to enhance temper resistance. It has been found that Si addition is beneficial in giving higher ultimate tensile strengths with ductility being improved or maintained.[8,13,14]

B. Ingot Preparation

Ingots of approximately 2-1/2" diam and 10" length, induction melted, were case in an inert atmosphere. These were then forged to 3/8" by 9/16" bars. Following forging the ingots were ground to 1/4" by 1/4" bar stock.

Bars of 4" length were austenitized at temperatures of 1093°C (2000°F) to 1200°C (2200°F) depending upon the composition of the steel.

No protective atmosphere was employed as the high chromium and nickel contents have the effect of conferring sufficient oxidation resistance to the steels at the temperatures used. An austenitizing time of one hour was employed for all steels. The bar stock was air cooled from the austenitizing temperature to room temperature and examined by metallograph and hardness measurements to insure that the samples were essentially 100% austenitic.

The compositions of the steels employed are given in Table I.

Table I

Code	Alloying Element, Weight%				
	C	Cr	Ni	Mo	Si
No. 62	0.69	5.02	13.57	---	---
No. 63	0.70	7.29	9.88	---	---
No. 51	0.23	2.94	21.46	---	---
6481	0.23	2.14	19.93	1.95	1.32
6473	0.46	4.68	13.68	2.00	1.47
A-1	0.23	4.68	14.98	1.97	1.92
A-2	0.47	5.63	9.97	1.94	1.90

C. Deformation Technique

The bar stock was cleaned of any scale formed during austenitizing by grinding. The bar was cut into short lengths and sealed in 1/2" diam 109 mm wall stainless steel tubing. The function of the tubing was to insure uniformity of temperature during the rolling operation.

The specimens were heated in a tube furnace prior to and during the rolling operation. A preheat time of 15 minutes was used prior

to the rolling operation in order to bring the stainless steel casing and the specimen up to the rolling temperature. The deformation process was carried out in steps of 25 mils per pass during the initial stages of deformation, and 15 mils per pass at the final stages of deformation. After every two passes through the rolling mills, the specimen was returned to the furnace for a period of approximately two minutes. An infrared pyrometer sighted on the specimen during rolling was employed to insure that the specimen temperature remained constant throughout the rolling operation. The total time for 80% reduction in thickness of the specimen was less than one hour. After the last pass through the rolling mill, the specimen was water quenched to retain the austenite phase at room temperature. The specimens were removed from the stainless steel jacket by cutting and samples were prepared for metallography.

Deformation temperatures of 400 °C, 450 °C, and 500 °C were employed.

D. Cyclic Heat Treatment

The specimens were heated to a preselected tempering temperature (cycle tempering temperature) followed by alternate quenching to decreasing cryogenic temperatures and intermediate tempering. Figure 1 shows a schematic representation of the thermo-mechanical treatment employed.

The heating medium for tempering was a molten salt bath of nitrates in a resistance heated container. Tempering temperatures of 450, 500, 600 and 625 °C were employed depending upon the steel composition. For the cryogenic treatment a mixture of ethanol and liquid nitrogen in suitable proportion was used. Liquid nitrogen was

added to the alcohol to reduce the temperature to successively lower values. An iron-constantan thermocouple was employed to measure the temperature of the cryogenic bath which was stirred frequently to minimize temperature gradients. Close temperature control was assured by employing a large amount of liquid and the use of fairly small specimens.

The specimens were heated to a constant tempering temperature for 10 minutes followed by quenching to the lower temperature and cryogenic treatment at the lower temperature for 5 minutes. The cycle was repeated nine times using a constant tempering temperature throughout and successively lower quenching temperatures. After the final quench the specimens were subjected to different tempering treatments.

E. Hardness and Metallographic Studies

The progress of the phase transformation was followed by hardness measurements after each quenching treatment.

A complete metallographic investigation was conducted. The specimens were first electropolished and then etched electrolytically.

F. Mechanical Testing

The steels which exhibited the best response to the thermo-mechanical treatment in terms of increase in hardness were tested for ductility in bend testing. A comparative evaluation of the ductility of the different alloys after the treatment was obtained. Three point bending was employed.

Final evaluation of the process was done by tensile testing. Tensile specimens 2" long and 1/8" thick were used (the specimen dimensions are shown in Appendix A). Tensile tests were conducted on an Instron machine using a crosshead travel speed of 0.1 cm/minute.

III. EXPERIMENTAL RESULTS

A. Variables

The different variables in the process are as follows: austenitizing temperature, deformation temperature and cycle tempering temperature. A summary of the variables used and their effect on the properties is given in Table II.

1. Austenitizing Conditions

Austenitizing temperatures of 1100 and 1200 °C were used for the low and high carbon steels respectively.

2. Deformation Temperature

To establish the optimum deformation temperature the alloys were deformed at temperatures of 400, 450, 500 and 550 °C. A uniform reduction of 80% thickness was employed. It was observed that the high carbon steels transformed excessively to pearlitic products at the higher deformation temperatures and cracked with about 60% deformation at deformation temperatures of 500 and 550 °C. Higher deformation temperatures yield austenites of higher hardness as seen in Figs. 2 and 3.

It was found that deformation at any temperature has the effect of stabilizing the austenite and lowering the M_s of the steel. It was observed that the first martensite appeared at temperatures of -50 to -60 °C while the designed M_s temperature was -30 to -40 °C for the alloys. Figure 4 shows the metallograph of one of the alloys after deformation.

3. Cycling Treatment

The purpose of the cycling treatment is to produce a suitable microstructure of such characteristics that enhanced properties result.

Table II

Variable kept constant throughout experiment	Process	Effect on hardness	Resulting microstructure
Austenitizing temperature	Austenitized and quenched to liquid nitrogen	Hardness higher than austenite	Figure 18
Austenitizing temperature, cycle tempering temperature	Austenitized and cycled (without deformation)	Hardness increases over austenitized and quenched alloy	Figure 19
Austenitizing temperature, deformation temperature	Austenitized, deformed and quenched to liquid nitrogen	Increased hardness over the prior two treatments	Figure 20
Austenitizing temperature, deformation temperature, cycle tempering temperature	Austenitized, deformed and cycled	Highest hardness	Figure 21

Effect of the different variables on the hardness and microstructure of high carbon alloy A-2.

A small amount of the austenite is transformed by cooling just below the M_s temperature and then reheated to an intermediate tempering temperature to temper the martensite. The process is repeated using decreasing cryogenic temperatures down to liquid nitrogen. Since diffusion rate is proportional to temperature and time to the one half power, the less important variable, time was held constant at ten minutes, while the temperature was varied to produce the desired alloy carbide precipitation.

Different cycle tempering temperatures were employed. Figures 5 and 6 show the effect of cycle tempering temperature on the hardness after quenching to successively lower temperatures below the M_s of two different alloys of different carbon contents.

In the 0.23% C-5% Cr-15% Ni-2% Mo-2% Si steel the higher tempering temperature (cycle) of 600°C yields the highest hardness (Fig. 5). The lower tempering temperature of 450°C does not have a very favorable effect on the hardness while a higher temperature of 625°C also yields a steel of inferior hardness.

In the high carbon alloy (0.47% C) the lower cycle tempering temperature of 450°C resulted in the highest hardness (Fig. 6). A 600°C tempering during the cycle drops the final hardness from R_c 57 (using a 450°C tempering temperature) to R_c 55. When a cycle tempering temperature of 625°C was used the hardness dropped catastrophically after three or four cycles.

B. Final Tempering

The set of alloys which had the highest hardness and best microstructure were employed for further investigation. These were (a)

0.23% C-5% Cr-15% Ni-2% Mo-2% Si henceforth referred to by the code A-1 and (b) 0.47% C-5.6% Cr-10% Ni-2% Mo-2% Si, referred to as A-2.

The treated alloys were tempered at different temperatures starting at 500°C and going up to 625°C for 15 minutes each at every temperature. To observe the effect of tempering on deformed austenite which has not been cycle transformed, samples of the same alloys austenitized and deformed were subjected to the same tempering treatment. The results are shown in Figs. 7 and 8. In the case of the low carbon alloy the specimen before tempering was cycle heat treated using a cycle tempering temperature of 450°C (which is not the optimum). This was done to detect any hardness peak obtained with increasing tempering temperature. With the high carbon steel A-2 the lowest temperature (450°C) was the optimum and the object of tempering this alloy was to discover if the hardness would increase any further. Previous results have indicated that lower tempering temperature of 450°C is the optimum for the low carbon steels A-1 (Fig. 6).

The results of final tempering indicate that the low carbon alloy exhibits a hardness peak at 550°C followed by a hardness drop while the high carbon alloy shows a drop in hardness with higher tempering temperatures.

To detect the effect of each of the different parameters of the process such as austenitizing, deformation and cyclic quenching, experiments were conducted on the alloys subjected to the different parameters to the exclusion of the others. Table II shows the variables used and resulting properties of the alloys employed. Table III gives the different hardness values obtained when two steels

Table III

	Process	Hardness (Rockwell C) A-1	A-2
1.	Austenitized and quenched to liquid nitrogen	25	43
2.	Austenitized and cycled (without deformation)	38	47
3.	Austenitized, deformed and quenched to liquid nitrogen	45	51
4.	Austenitized, deformed and cycled (complete thermo-mechanical treatment)	49	57

Effect of process variables on the hardness of two steels.

Table IV

Alloy and Process History	Yield Strength psiX10^{-3} (0.2% offset)	Tensile Strength psiX10^{-3}	Reduction of area %	Elongation %
A-1 deformed 80% at 400°C, cycled. Cycle tempering temperature - 600°C	197	242	37	26
	201.2	261	37	26
	206.6	276.1	36	27
Same treatment as above with a final temper at 600°C 30 minutes	157.1	247.1	38	28
A-2 deformed 80% cycled. Cycle tempering temperature 450°C	229.1	286.6	14	16
	220.1	290	15	16
	235.7	281.1	15	15
Same as above with a final temper at 550°C for 15 minutes	182.4	340.5	13	14
Same as above with a final temper at 550°C for 30 minutes	172.7	330.96	-	19

of differing carbon contents are subjected to the various treatments in Table II.

C. Tensile Data

Dimensions of the tensile specimens used are given in Appendix A.

Table IV gives the tensile, yield, and ductility data of a number of specimens of the alloys of different carbon content. The effect of tempering on the strength values is also shown.

Table V gives a comparison of the mechanical properties of alloys with and without Si and Mo in their composition.

Table V

Alloy and Process History	Yield Strength psi 10^{-3} (0.2% offset)	Tensile Strength psi 10^{-3}	Elongation %
No. 51--Deformed 80% at 450°C cycled. Cycle tempering temperature-500°C.	176	192.5	15
No. 62--Deformed 80% at 450°C cycled. Cycle tempering temperature-500°C.	218.2	270.9	9
No. 63--Deformed 80% at 450°C cycled. Cycle tempering temperature-500°C.	142.2	186.8	8
A-1--Deformed 80% at 400°C cycled. Cycle tempering temperature-600°C.	206.6	247.1	28
A-2--Deformed 80% at 600°C cycled. Cycle tempering temperature-450°C.	235.7	281.1	15

IV. DISCUSSION

A. Effect of Cycling Treatment

A small amount of martensite is produced with each low temperature quench. The formation of martensite is accompanied by a volume change. This leads to dislocations being produced in the untransformed austenite. These dislocations act as nucleating sites for carbide formation which is also facilitated by the tempering treatment between quenches.

The cycle tempering temperature has a significant effect on the properties. Lower temperatures are found to be suitable for optimum results with high carbon steels while higher temperatures yield good results with low carbon alloys. The lower temperatures in the case of low carbon steels is not high enough to induce carbide precipitation while the high temperature above the optimum overages the carbide leading to a fall in hardness and hence strength. The high carbon alloys showed a drop in strength at higher cycle tempering temperatures, being due to excessive carbide agglomeration.

Figure 11 shows a micrograph of deformed austenite cycle quenched down to -120°C in a high carbon steel (A-2). Uniform carbide distribution is evident. The lighter regions are probably composed of as yet untransformed austenite. This picture represents the microstructure about half way through the cyclic quench treatment. Figures 12 and 13 show micrographs of the same steel after complete cyclic treatment, the two pictures being of the same region at different magnifications. It is observed that the amount of retained austenite is reduced to a small value. Almost complete transformation is observed.

Figures 14 and 15 are micrographs of the low carbon steel (A-1) at

different magnification. The low carbon content has resulted in a microstructure with a large percentage of untransformed austenite with carbides formed along dislocation bands produced during deformation. The high percentage of untransformed austenite is due to the M_f temperature of the steel being below the temperature of liquid nitrogen. Another factor that might be responsible for the retention of austenite is the stabilization effect that deformation has upon the austenite.

Figures 16 and 17 are micrographs of two other steels investigated (Fig. 16--Steel No. 51; Fig. 17--Steel No. 62). The micrographs show the structure of the steels after being subjected to the complete thermomechanical treatment. These steels do not contain Si or Mo and had inferior mechanical properties to those containing Si and Mo (Figs. 1 and 2). These micrographs show non-uniform carbide distribution when compared to those alloys containing Si and Mo.

The third set of alloys investigated (Nos. 81 and 73) did not react very favorably to the treatment although the composition of these steels was substantially the same as another set which were the best alloys among all the compositions investigated. However, the difference in composition is shown in the higher nickel contents which could be the reason for the low hardness obtained. Nickel lowers the m_f of the alloy.

A high carbon alloy (No. 63) investigated resulted in cracking during deformation due to excessive grain boundary agglomeration of the carbides. The high carbon content may also lead to the formation of iron carbides rather than the stronger and relatively temperature insensitive alloy carbides.

Cycling is the significant parameter of this process. The M_f

temperatures of the alloys lie at very low values. As such, a direct quench to liquid nitrogen following deformation will not result in complete or even a significant amount of transformation of the austenite to martensite. Heterogeneous nucleation is facilitated by the very high dislocation density in the austenite following deformation. Transformation to martensite further increases the dislocation density due to the plastic deformation of the austenite by the volume expansion of the transformation reaction. This process which could be termed "internal cold working" increases dislocation density and hence prevents the formation of agglomerated carbides by providing more nucleation sites.

It is evident from a study of the microstructure that the cycling process has the designed effect of forming a small amount of martensite at a time, the plates being confined within the dislocation network. The martensite is tempered along with the austenite still remaining untransformed which decomposes to pearlitic products at the high temperatures.

B. Final Tempering

The deformed but uncycled samples showed an increase in hardness with increasing tempering temperature. This is due to the austenite decomposing to pearlitic transformation products. However, the highest hardness obtained in these specimens is lower than the hardness of the alloys which have gone through the cyclic treatment. This follows logically from the fact that the microstructures in the two cases are very different due to the different modes of formation of the carbides.

High temperature tempering (625°C) of the low carbon alloy (A-1) has an adverse effect upon the properties while the same alloy when

subjected to the same high temperature tempering while in the austenitic condition (deformed austenite) without cycling, increases the hardness which is retained at the high temperature. The increase in hardness of the deformed austenite is due to the transformation of austenite to transformation products of the pearlitic type. To explain the instability of the deformed and cycled alloy as opposed to the stability of the deformed but uncycled alloy (Figs. 3 and 5) during high temperature tempering, it is postulated that the tempered martensite in the deformed and cycled alloy reverts back to austenite at high tempering temperatures thus leading to a drop strength. The carbides in the deformed, uncycled and tempered alloy consist of pearlitic products which do not revert back to austenite at these temperatures. However these carbides although stable at high temperatures have very inferior microstructural features and hence lead to poor strength.

C. Variables

The different variables in the process have a significant effect upon the properties of the steels. The effect of each variable on the alloy was examined while the others were kept constant.

The alloys were austenitized and quenched to liquid nitrogen. The hardness obtained in this case was found to be much less than that of the deformed and cycled alloy. Figure 18 is a microstructure of the high carbon alloy austenitized and quenched, showing the martensite structure.

The austenitized and deformed alloy was quenched to liquid nitrogen. Deformation increases the hardness of the alloy considerably but the hardness is still lower than that obtainable from deformation combined

with cycling. Figure 19 shows a microstructure of the low carbon alloy after deformation and quenching. The martensite plates are seen broken up by the dislocation bands. The familiar "lightening bolt" morphology of the martensite is evident. This can be understood in terms of the break-up of continuity of the austenite lattice by multiple slip resulting from deformation of the austenite. If a moving martensite plate is to continue to propagate along the same orientation it starts with whenever it crosses a dislocation band in austenite, it will have to be displaced. In some cases the discontinuity may be too much for the plate to continue so a new plate will be propagated but displaced from the original. Also any precipitation on slip bands may stop martensite plates from propagating.

The third parameter, namely cycling, was isolated from deformation by cycling an austenitized sample of the steel without prior austenite deformation. The hardness obtained was intermediate between the direct quenched alloy and the deformed and quenched alloy. The effect of deformation on hardness is seen to be considerable. Cycling the alloy furnishes a higher hardness than direct quenching. This is probably due to more of the carbon being drawn out of solution in austenites by the alternate quenching and tempering of the cycling process. It is hence seen that the combination of austenite deformation and cyclic heat treatment is a potent mechanism for strengthening steels. Figure 20 is a microstructure of the high carbon alloy (A-2) austenitized, deformed, cycled and tempered.

D. Tensile Testing

The best combination of strength and ductility is obtained in

those alloys which contained Si and Mo.

With the high carbon steels (A-2) it was observed that the stress-strain curves were serrated beyond the yield point. These serrations form during repeated yielding following the yield point on the stress-strain curve. The serrations could be due to the transformation of retained austenite to martensite during straining. The transformation to martensite is accompanied by a volume change which is reflected in a load drop on the stress-strain curve.

In order to reduce the content of retained austenite, the alloys were tempered for 15 minutes and 30 minutes, at 550°C for the high carbon alloy and at 600°C for the low carbon alloy.

In the high carbon alloy a 15 minute temper increased the tensile strength to a value of 340,500 psi with a drop in yield strength to 182,000 from a value of 235,700 psi. A slight drop in ductility is observed. Tempering for half an hour decreases both the yield and tensile strengths with an increase in ductility. The low carbon steel reacted unfavorably to tempering with a decrease in strength as shown in Figs. 9 and 10. Figures 22 and 23 are microstructures of the high carbon steel after ausforming, cycling and tempering for 15 minutes. The two microstructures are of the same region at two different magnifications. Figure 24 shows the effect of tempering for 30 minutes on the same steel.

Figure 25 shows the microstructure of the low carbon steel following tempering for 30 minutes. The microstructure reflects the inferior properties of this steel when tempered.

Tempering the high carbon steel did not completely eliminate the serrations along the stress-strain curve although fewer serrations were

observed. This factor raises the possibility that the high carbon steels are exhibiting the phenomena known as the Portevin-Le Chatelier effect (repeated yielding). This is a series of decreasing load drops on a rising stress-strain curve which cease when the specimen starts to neck down at instability.[9,12] It has been observed that alloys with austenites with the greatest strain hardening coefficients are those which produce the strongest martensites. These are alloys exhibiting the Portenvin-Le Chatelier effect. This effect is associated with a strong interaction between dislocations and strain induced precipitates formed during deformation. It is assumed that strain enhanced formation of vacancies sufficiently increase the diffusion rate of substitutional atoms to form small, finely dispersed, alloy carbide particles. Once the alloy carbides form a critical dispersion, they act as a barrier to glide, leading to dislocation multiplication and yielding.

The effect of Si and Mo on the strength of the alloys is significant. Three alloys of different carbon contents and not containing Mo or Si were tested. A comparative study of the results are shown in Table V. It is observed that Si and Mo increase the strength and ductility of the alloys.

V. SUMMARY

A summary of the results of the investigation may be set forth as follows:

Direct quench of the austenitized alloys to liquid nitrogen does not increase the hardness significantly. Cycling the alloys and sequentially transforming the austenite to martensite has a favorable effect on the hardness. Transforming deformed austenite to martensite by direct quenching results in a steel with a higher hardness than that obtained by direct quenching undeformed austenite. The combination of deformation and cyclic transformation of the austenite results in a significant improvement in mechanical properties.

Low cycle tempering temperatures for high carbon steels and high cycle tempering for low carbon steels are found to result in optimum properties.

Final tempering for short periods at temperature increased the tensile strength but decreased the yield strength of the high carbon steels. Longer tempering times were detrimental to the properties. The low carbon steels reacted unfavorably to tempering showing a drop in strength.

Alloy composition is found to be a critical factor in the process. Steels not containing strong carbide formers like Mo did not respond very favorably to the treatment. Alloys with Mo and Si in their composition had the best properties following the complete treatment.

Untransformed austenite was observed both in the low and high carbon steels. Austenite retention was considerable in the low carbon steels. The high carbon alloys exhibited a serrated stress-

strain curve showing austenite transforming to martensite as a result of the applied strain. No serrations were observed in the stress-strain curves of the low carbon steels.

The optimally treated steels had yield strengths in excess of 200,000 psi with greater than 28% ductility (elongation) for the low carbon alloys (A-I) and greater than 220,000 psi yield and greater than 300,000 psi tensile strength with ductilities in excess of 12% (elongation) for the high carbon steels (A-2).

ACKNOWLEDGEMENTS

The author wishes to express his grateful appreciation to Professor E. R. Parker and Dr. V. F. Zackay, Department of Mineral Technology, University of California, for their guidance, encouragement and support throughout the course of this investigation.

This work was performed under the auspices of the United States Atomic Energy Commission through the Inorganic Materials Research Division of the Lawrence Radiation Laboratory.

References

1. M. Cohen, JISI, 201, 833 (1963).

2. J. E. Bailey, Electron Microscopy and Strength of Crystals, ed. G. Thomas and J. Washburn (Interscience Publications, New York, 1963) p. 535.

3. V. F. Zackay and E. R. Parker, in High Strength Materials, (John Wiley and Sons, Inc., New York, 1965) chapter 4.

4. V. F. Zackay and W. M. Justusson, "High Strength Steels", ISI Special Report 76, 14 (1962).

5. R. Phillips and W. E. Duckworth in High Strength Materials, (John Wiley and Sons, Inc., New York, 1965) chapter 7.

6. A. J. McEvily and R. H. Bush, Trans. ASM 55, 654 (1962).

7. A. J. McEvily, R. H. Bush, F. W. Schaller and D. J. Schmatz, Trans. ASM 56, 735 (1963).

8. W. E. Duckworth, P. R. Taylor and A. D. Leak, JISI 202, 205 (1964).

9. G. Thomas, D. Schmatz, and W. Gerberich, in High Strength Materials (John Wiley and Sons, Inc., New York, 1965) chapter 7.

10. D. J. Schmatz, F. W. Schaller and V. F. Zackay, The Relation Between Structure and Mechanical Properties of Metals, National Physical Laboratory Symposium No. 15 (Her Majesty's Stationery Office, London, 1963).

11. ASTM Special Technical Publication 48-M2, X-Ray Powder Data File, (American Society for Testing Materials, Philadelphia, Pennsylvania, 1963).

12. O. Johari, UCRL-11861 (unpublished work).

13. A. D. Hopkins and M. J. Ray, Metal Treatment 30.

14. W. E. Duckworth and P. R. Taylor, BISRA Report MG/Cont/23/64.

FIGURE CAPTIONS

Fig. 1 Schematic representation of the thermo-mechanical treatment employed. Associate microstructures at the different stages are shown at the top.

Fig. 2 Effect of deformation temperature on the hardness of a 0.23% C-3% Cr-21.5% Ni steel after quenching to successively lower temperatures below the M_s. The steel was austenitized at 1100°C and tempered at a temperature of 500°C.

Fig. 3 Effect of deformation temperature on the hardness of a 0.47% C-5% Cr-14% Ni steel after quenching to successively lower temperatures below the M_s. The steel was austenitized at 1200°C, and tempered at a temperature of 500°C.

Fig. 4 Effect of cyclic tempering temperature on the hardness of a 0.23% C-5% Cr-15% Ni-2% Mo-2% Si steel after quenching to successively lower temperatures below the M_s. The steel was austenitized at 1200°C, and deformed at a temperature of 600°C.

Fig. 5 Effect of cyclic tempering temperature on the hardness of a 0.47% C-5.6% Cr-10% Ni-2% Mo-2% Si steel after quenching to successively lower temperatures below the M_s. The steel was austenitized at 1200°C, and deformed at a temperature of 600°C.

Fig. 6 Effect of final tempering temperature on the hardness of a 0.23% C-5% Cr-15% Ni-2% Mo-2% Si alloy after quenching cyclically and on the hardness of an uncycled specimen subjected to 80% deformation. The steel was austenitized at 1200°C and deformed at a temperature of 400°C.

Fig. 7 Effect of final tempering temperature on the hardness of a 0.47% C-5.6% Cr-10% Ni-2% Mo-2% Si steel after quenching cyclically and on the hardness of a deformed but uncycled specimen. The steel was austenitized at 1200°C and deformed at a temperature of 600°C.

Fig. 8 Effect of tempering time at temperature on the tensile and yield strengths and on the ductility of a 0.23% C-5% Cr-15% Ni-2% Mo-2% Si alloy deformed and cycle quenched. The steel was austenitized at 1100°C and deformed at a temperature of 600°C. The cycle tempering temperature was 600°C. The final tempering was at a temperature of 600°C.

Fig. 9 Effect of tempering time at temperature on the strength and ductility of a 0.47% C-5.6% Cr-10% Ni-2% Mo-2% Si alloy deformed and cycle quenched. The alloy was austenitized at

1200°C and deformed at a temperature of 600°C. Cycle tempering temperature was 450°C and the final tempering temperature was 550°C.

Fig. 10 Deformed austenite showing slight carbide precipitation in the grain boundaries in a 0.47% C-5.6% Cr-10% Ni-2% Mo-2% Si alloy. The steel was deformed at 600°C. Magnification 250x.

Fig. 11 Deformed austenite cycle quenched down to -120°C in a 0.47% C-5.6% Cr-10% Ni-2% Mo-2% Si alloy. The steel was deformed at 600°C. Cycle tempering temperature was 450°C. Magnification 250x.

Fig. 12 Deformed austenite cycle quenched to liquid nitrogen in a 0.47% C-5.6% Cr-10% Ni-2% Mo-2% Si steel. The steel was deformed at 400°C. The cycle tempering temperautre was 450°C. Magnification 250x.

Fig. 13 Same alloy and treatment as in previous micrograph at a higher magnification. Magnification 1000x.

Fig. 14 Deformed austenite of a 0.23% C-5% Cr-15% Ni-2% Mo-2% Si steel cycle quenched to liquid nitrogen. The steel was deformed at 400°C using a cycle tempering temperature of 600°C. Magnification 250x.

Fig. 15 Same alloy and treatment as in previous micrograph at a higher magnification. Magnification 1000x.

Fig. 16 Austenite deformed and cyclically treated. Alloy composition 0.73% C-3% Cr-21.5% Ni. Austenitized at 1100°C. The steel was deformed at 450°C. Cycle tempering temperature was 500°C. Magnification 250x.

Fig. 17 Austenite deformed and cyclically quenched. Alloy composition 0.49% C-5% Cr-14% Ni. Austenitized at 1200°C. Steel deformed at 450°C. Cycle quenching temperature was 500°C. Magnification 250x.

Fig. 18 Steel austenitized at 1200°C and quenched to liquid nitrogen. Alloy composition was 0.47% C-5.6% Cr-10% Ni-2% Mo-2% Si. Magnification 250x.

Fig. 19 Steel austenitized at 1100°C, deformed at 400°C and quenched to liquid nitrogen. The alloy composition was 0.23% C-5% Cr-15% Ni-2% Mo-2% Ni. Magnification 250x.

Fig. 20 Undeformed austenite cycle quenched to liquid nitrogen. Cycle tempering temperature was 450°C. The alloy composition was 0.47% C-5.6% Cr-10% Ni-2% Mo-2% Si. Magnification 250x.

Fig. 21 Deformed austenite cycle quenched to liquid nitrogen in a 0.47% C-5.6% Cr-10% Ni-2% Mo-2% Si steel. The steel was

deformed at 400°C. Cycle tempering temperature was 450°C. Magnification 250x.

Fig. 22 Deformed austenite cycle quenched and tempered for 15 minutes at 500 C. The alloy composition was 0.47% C-5.6% Cr-10% Ni-2% Mo-2% Si. The steel was deformed at a temperature of 400°C and the cycle tempering treatment was 450°C. Magnification 250x.

Fig. 23 Same alloy and treatment as in previous micrograph at a higher magnification. Magnification 1000x.

Fig. 24 Austenite is deformed and cyclically quenched followed by tempering treatment for 30 minutes at 550°C. The alloy composition was 0.47% C-5.6% Cr-10% Ni-2% Mo-2% Si. The steel was deformed at a temperature of 400°C the cycle tempering temperature was 450°C. Magnification 250x.

Fig. 25 Austenite is cyclically quenched followed by a tempering temperature treatment for 30 minutes at 600°C. The alloy composition was 0.23% C-5% Cr-15% Ni-2% Mo-2% Si. The steel was deformed at a temperature of 400°C and the cycle tempering temperature was 600°C. Magnification 250x.

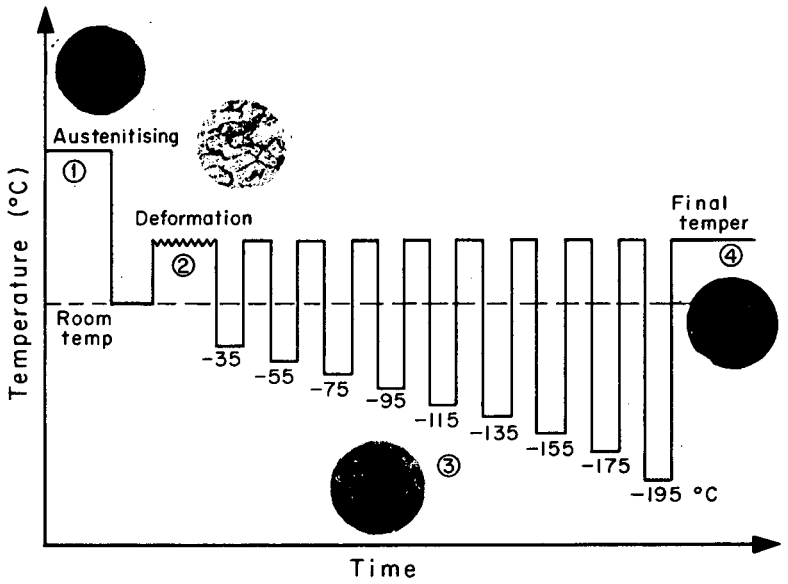

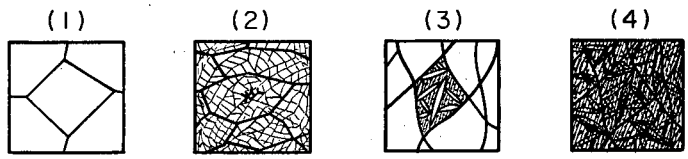

Austenite grains

Heavy slip band grid in austenite. Elongated grains.

Martensite plates confined by slip bands. High dislocation density with carbide precipitation.

Final structure

MU-35950

Fig. 1

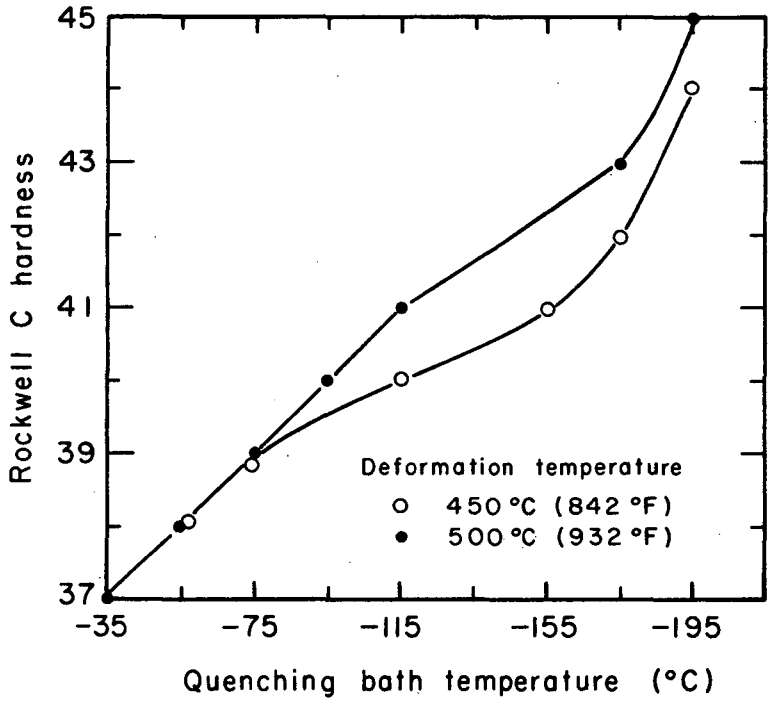

MU-35942

Fig. 2

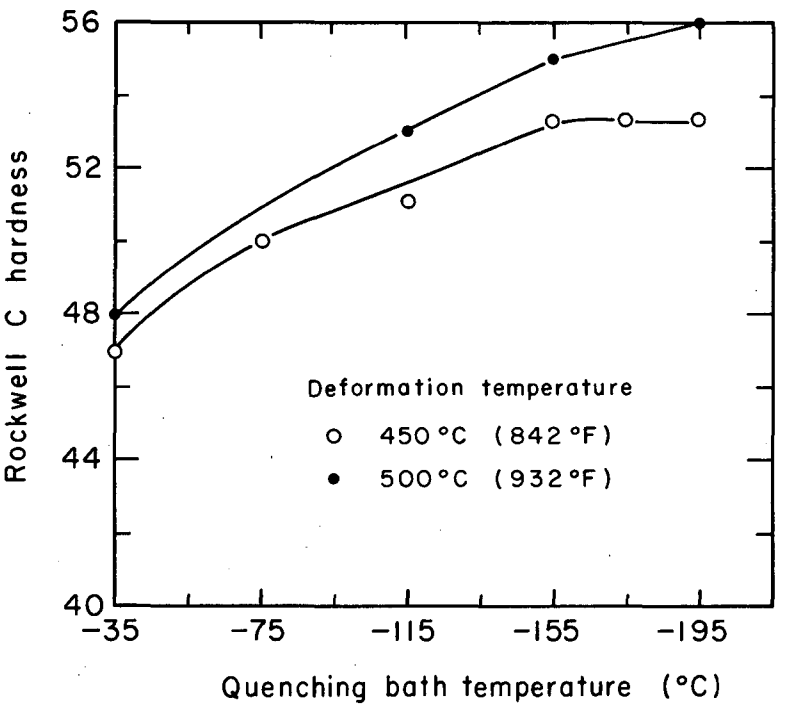

MU-35943

Fig. 3

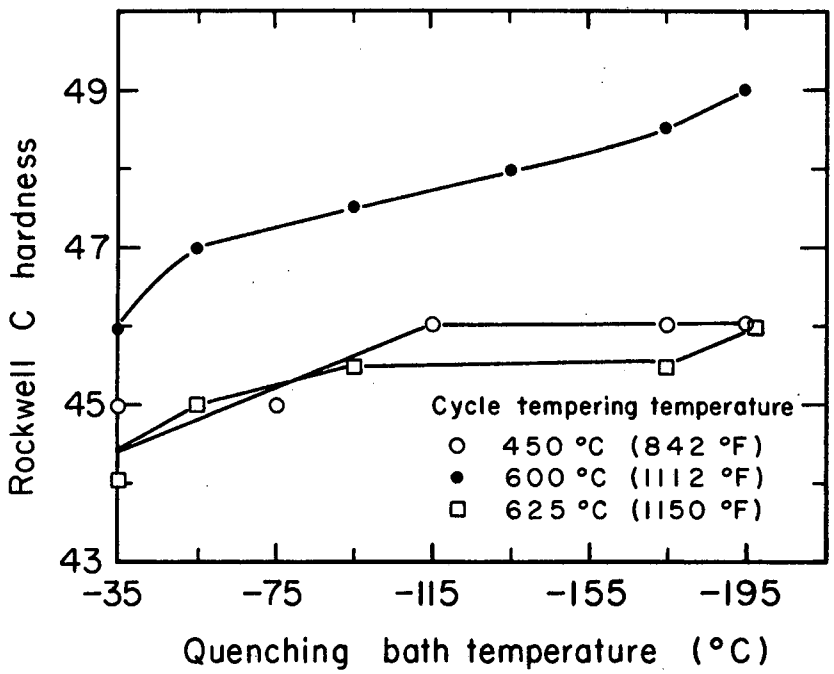

MU-35944

Fig. 4

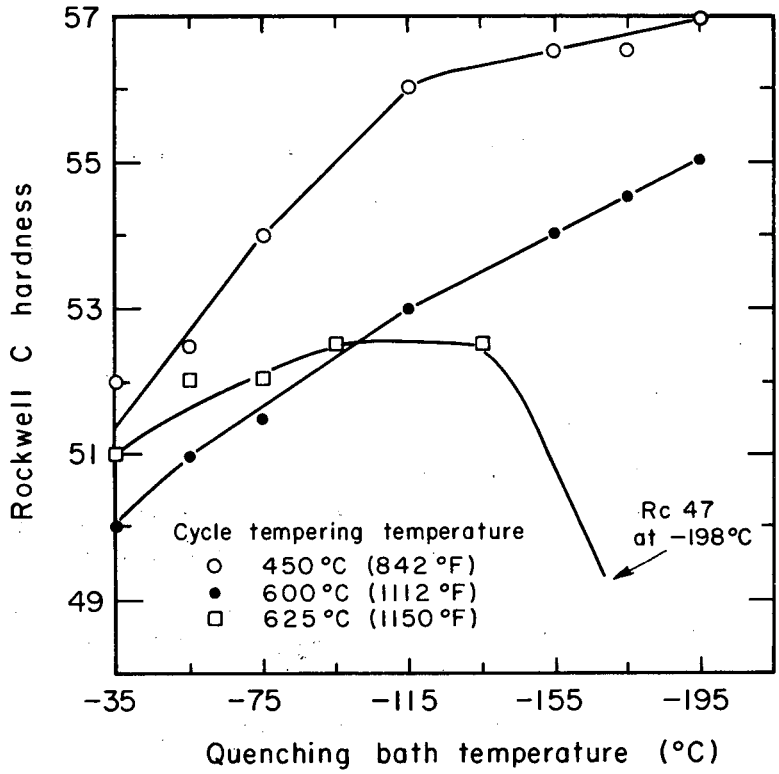

MU-35945

Fig. 5

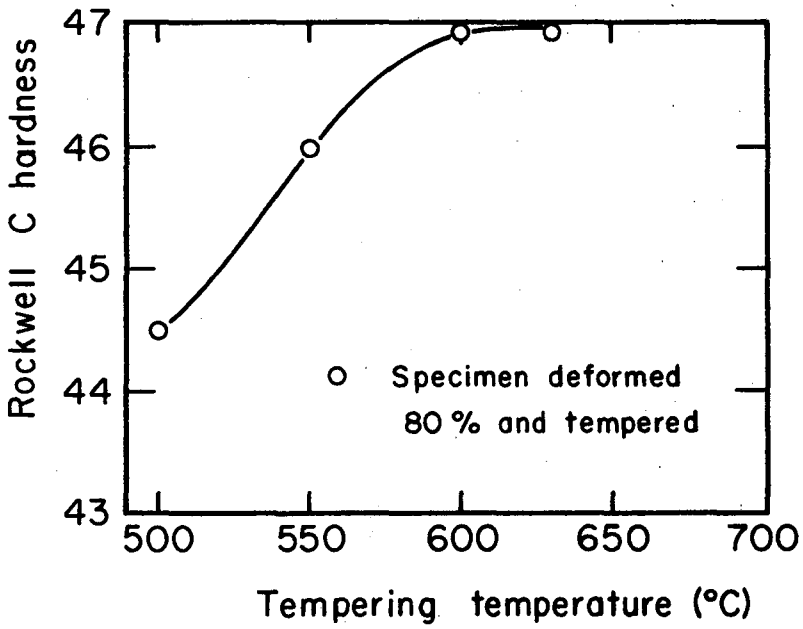

MU-35946

Fig. 6

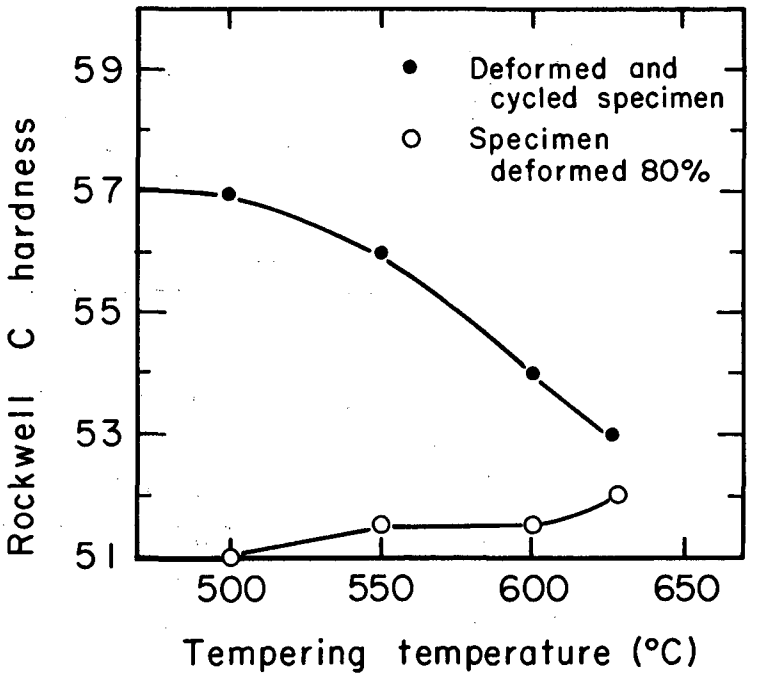

MU-35947

Fig. 7

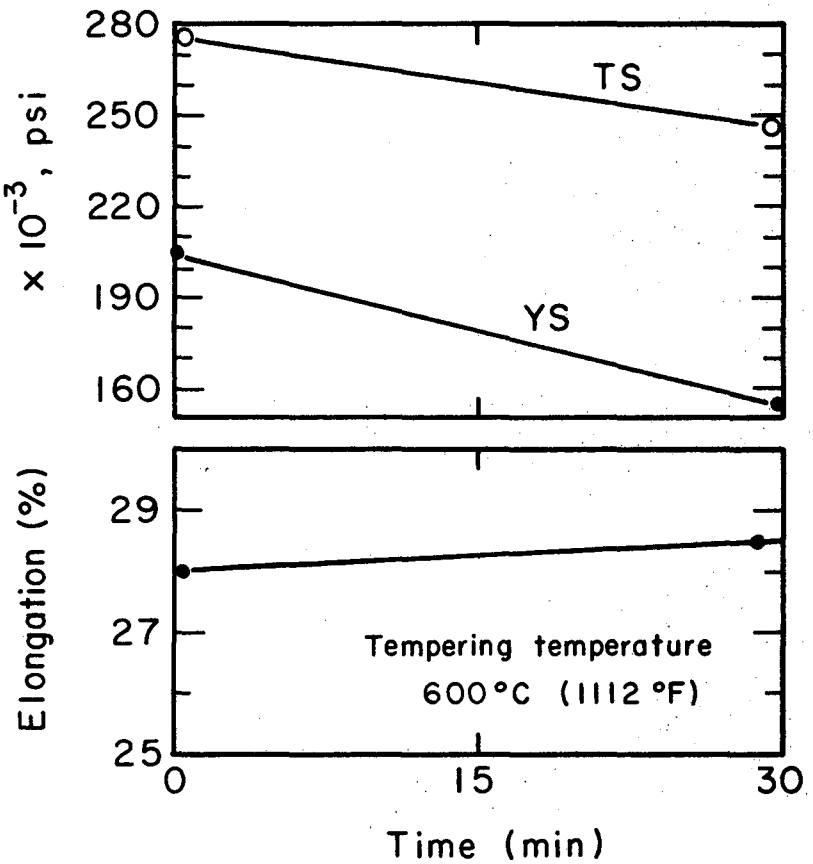

MU-35948

Fig. 8

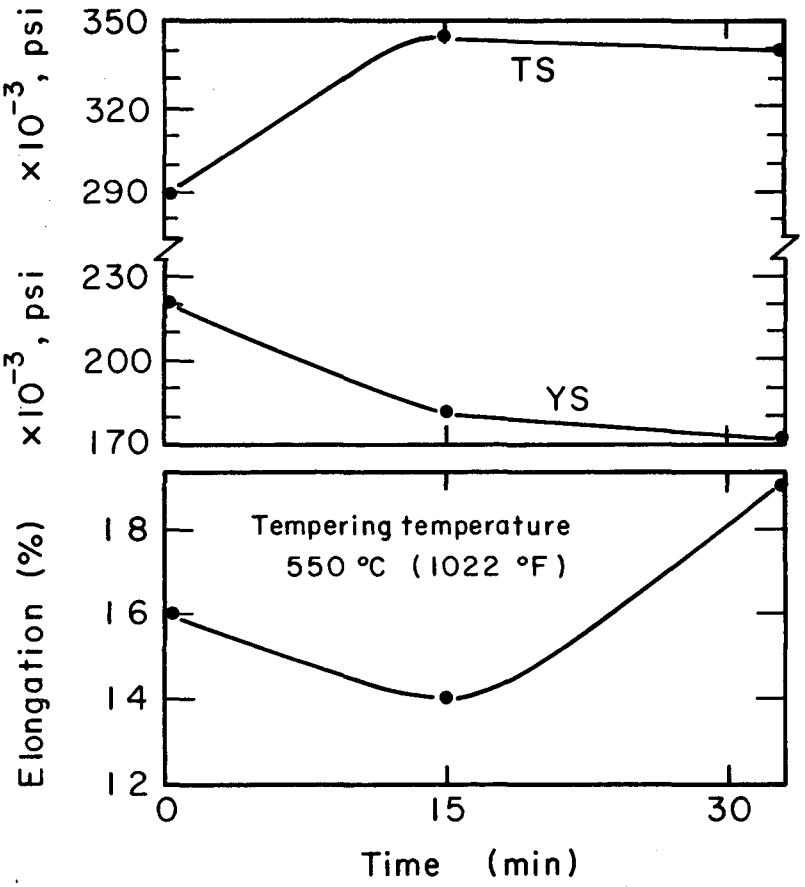

MU-35949

Fig. 9

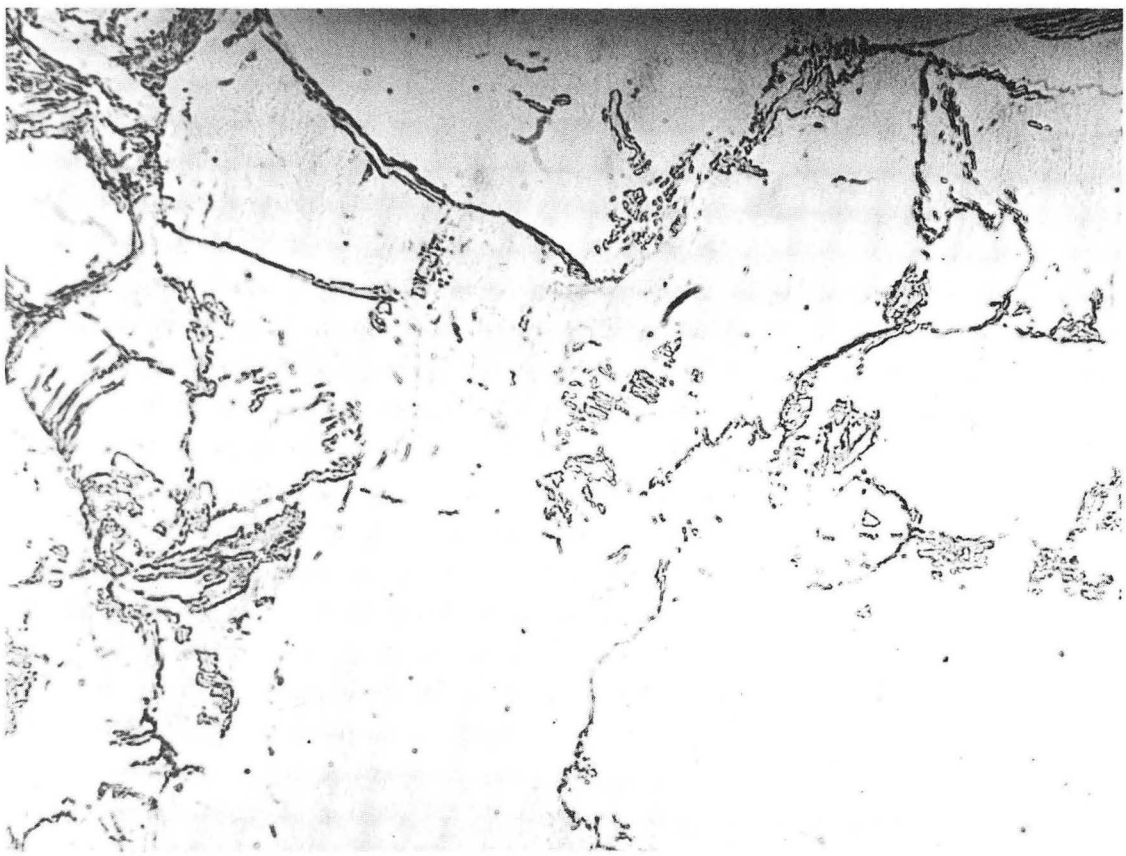

ZN-4955

Fig. 10

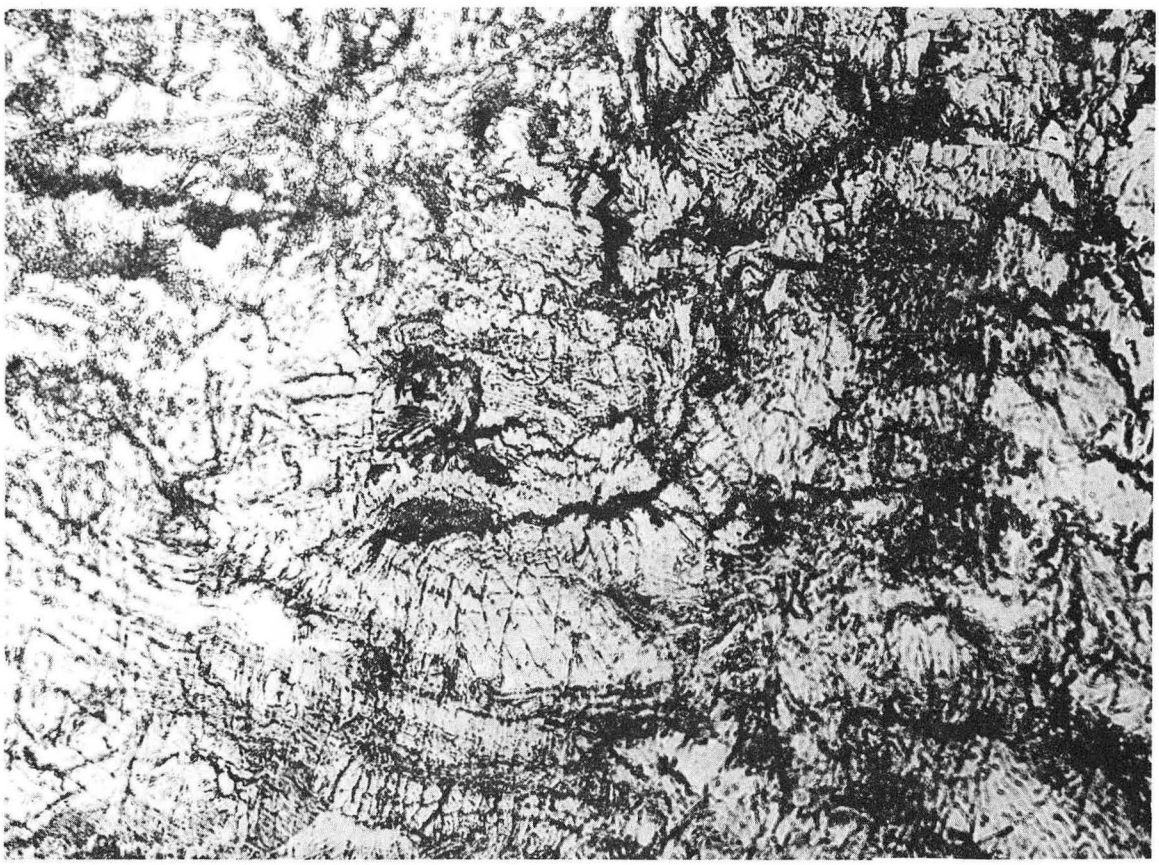

ZN-4945

Fig. 11

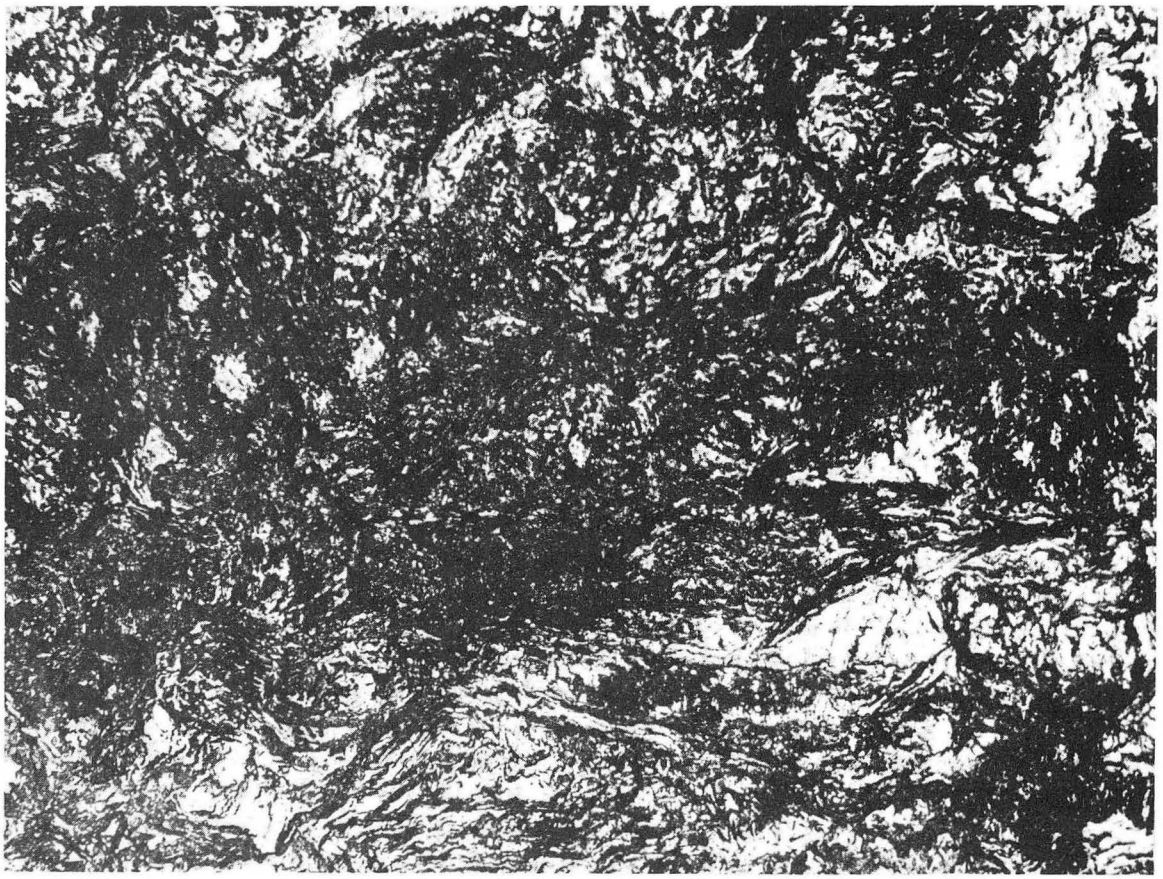

ZN-4940

Fig. 12

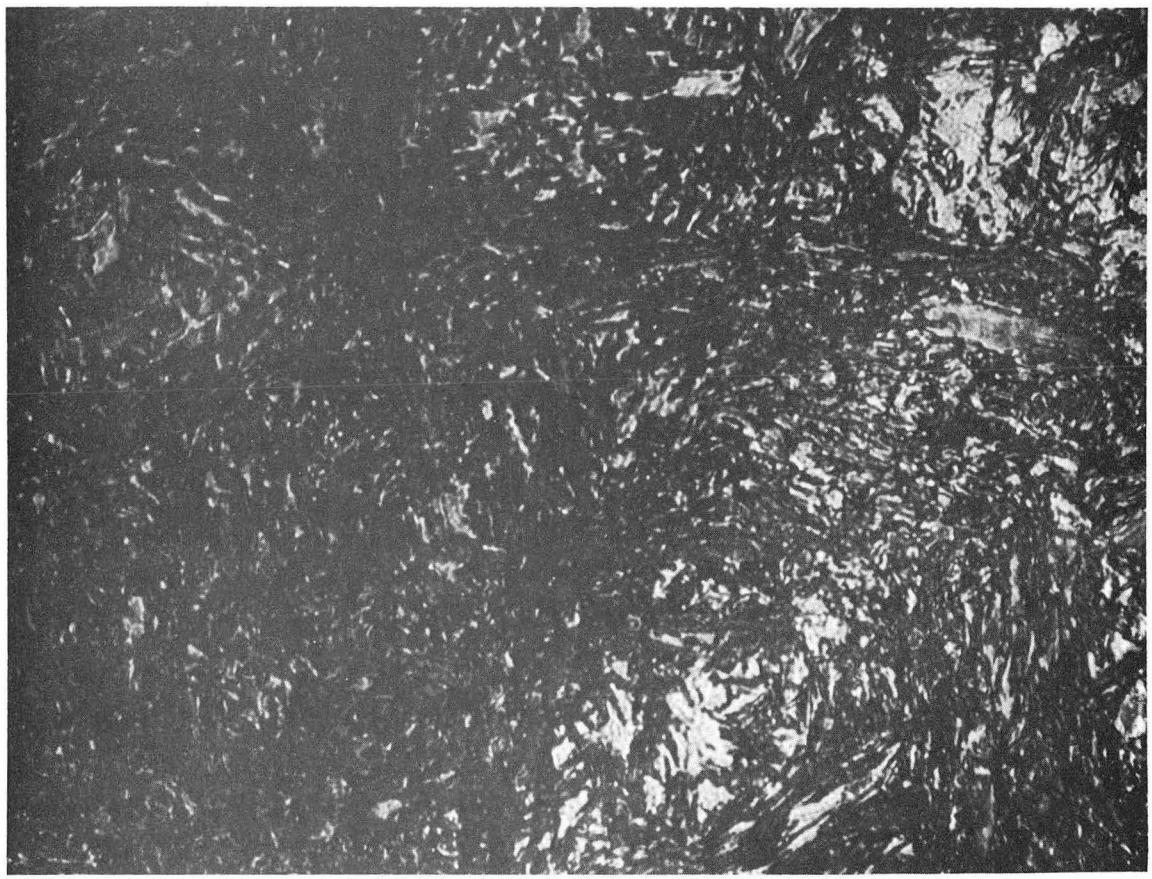

ZN-4942

Fig. 13

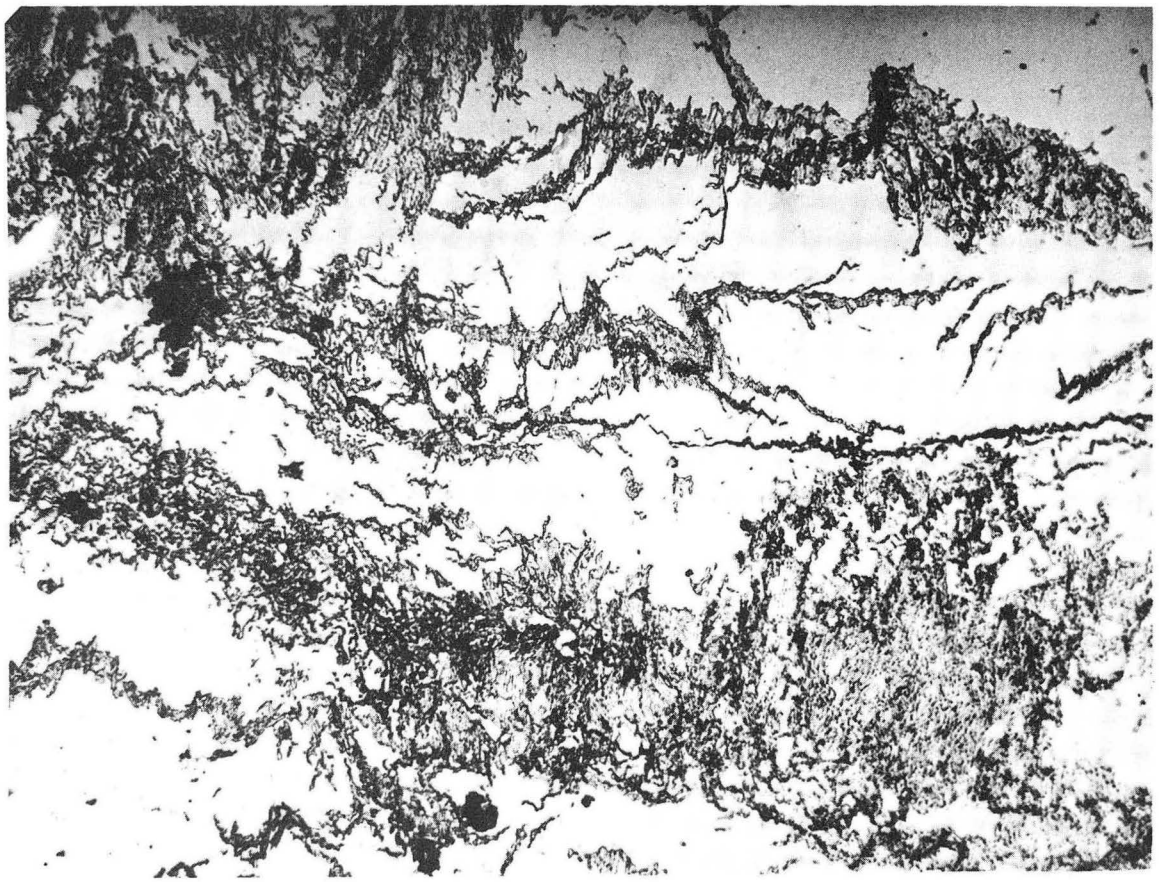

ZN-4943

Fig. 14

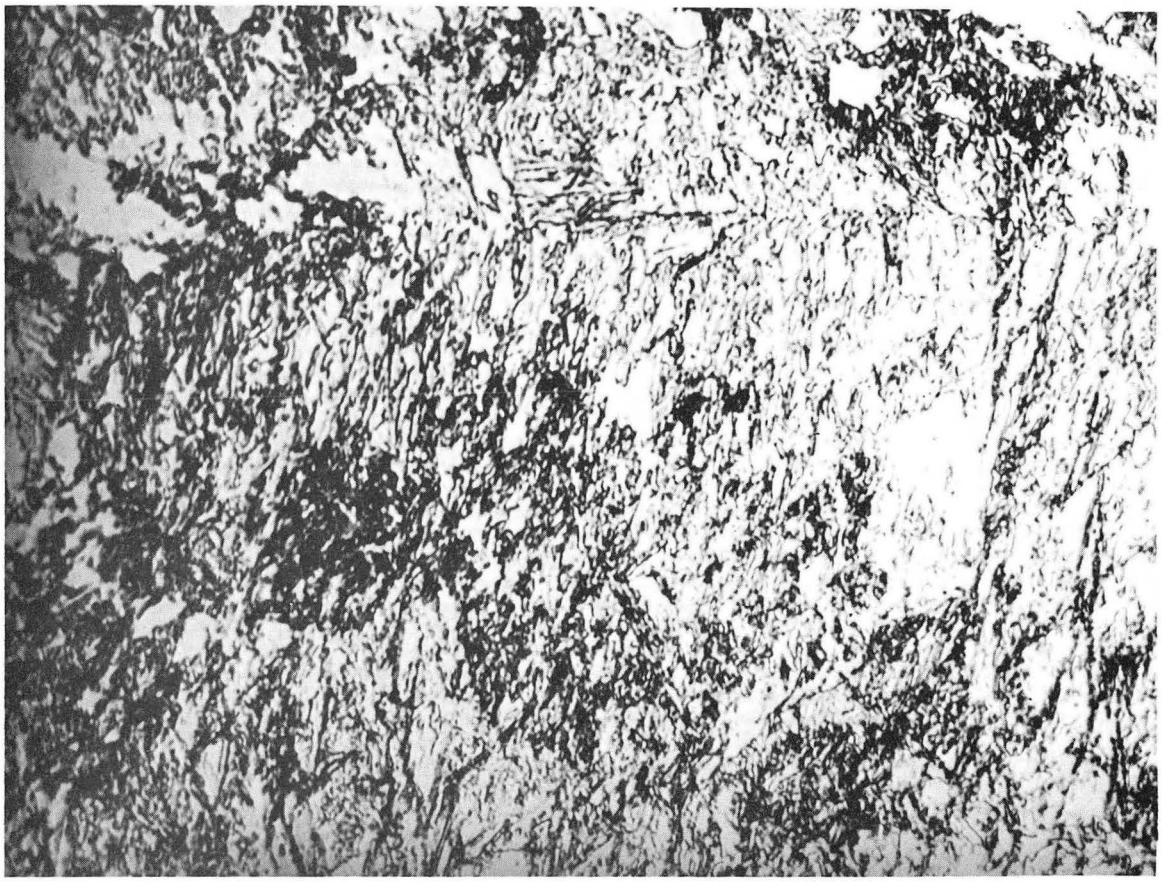

ZN-4944

Fig. 15

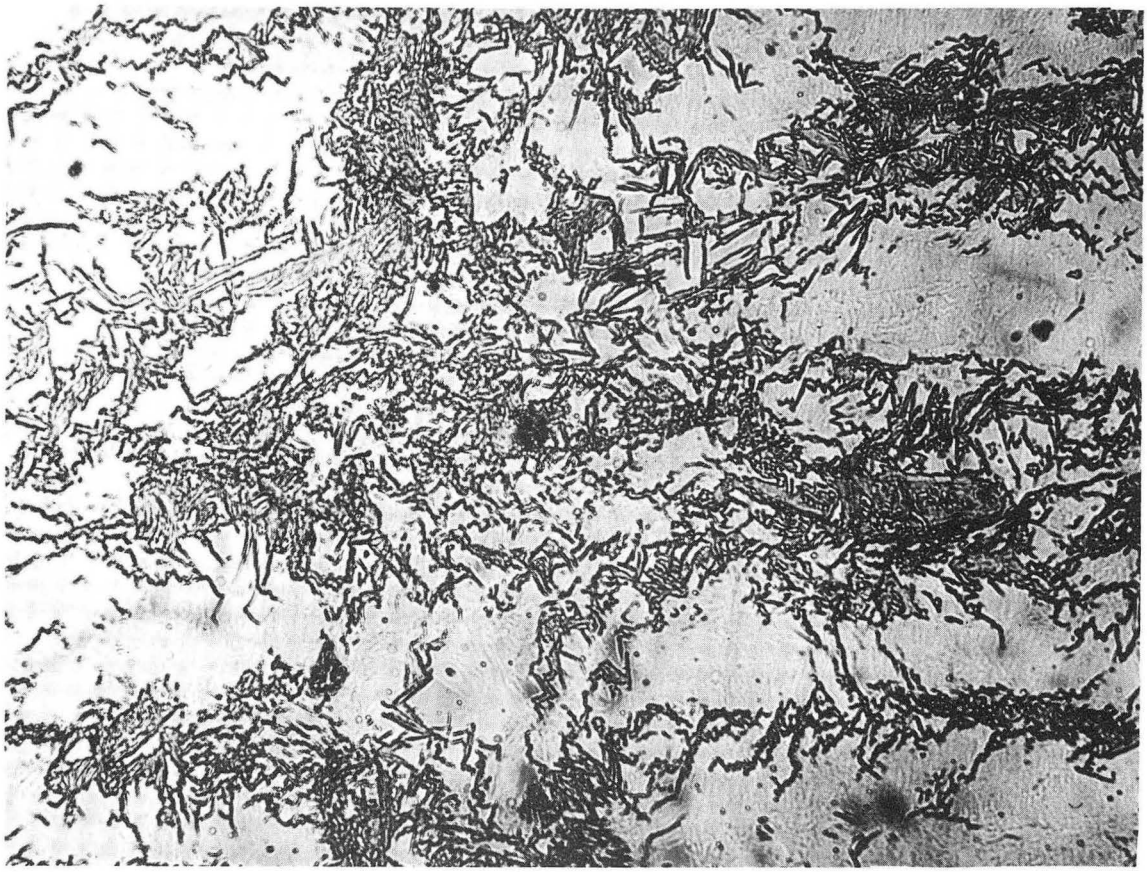

ZN-4951

Fig. 16

ZN-4950

Fig. 17

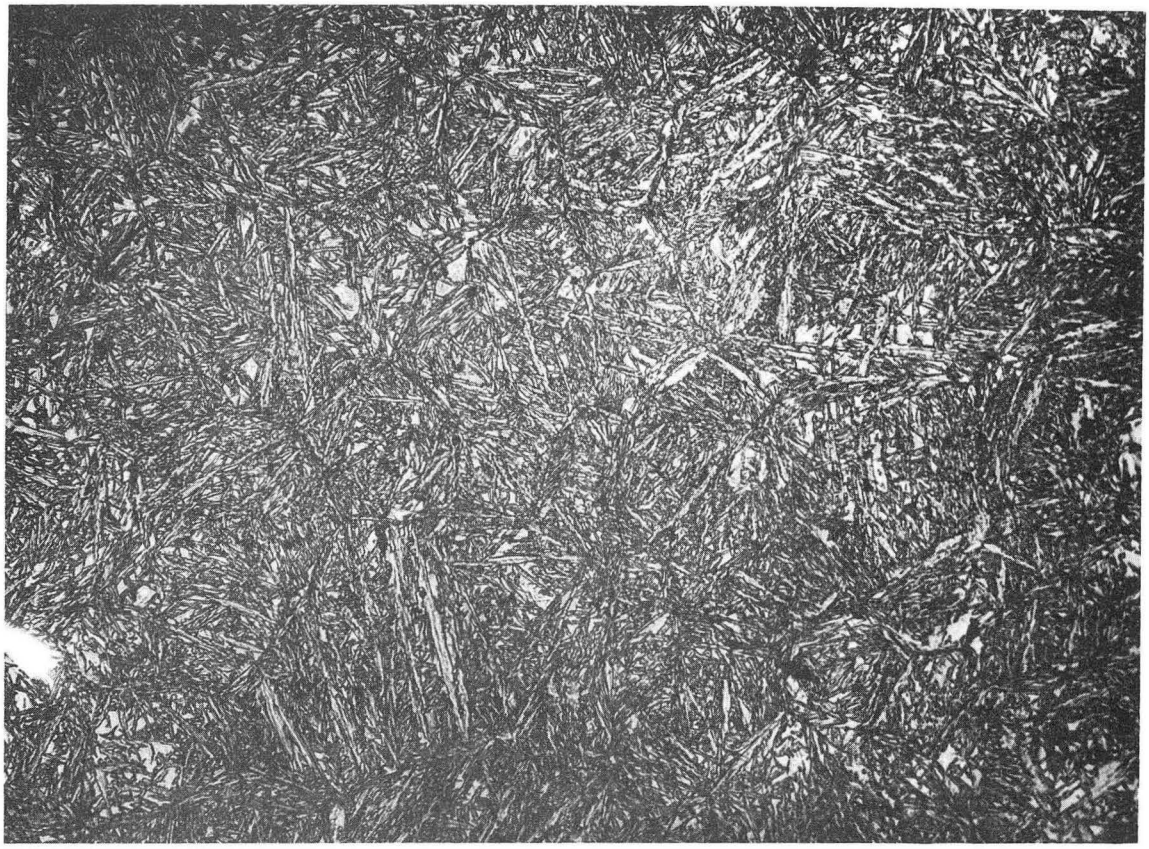

ZN-4953

Fig. 18

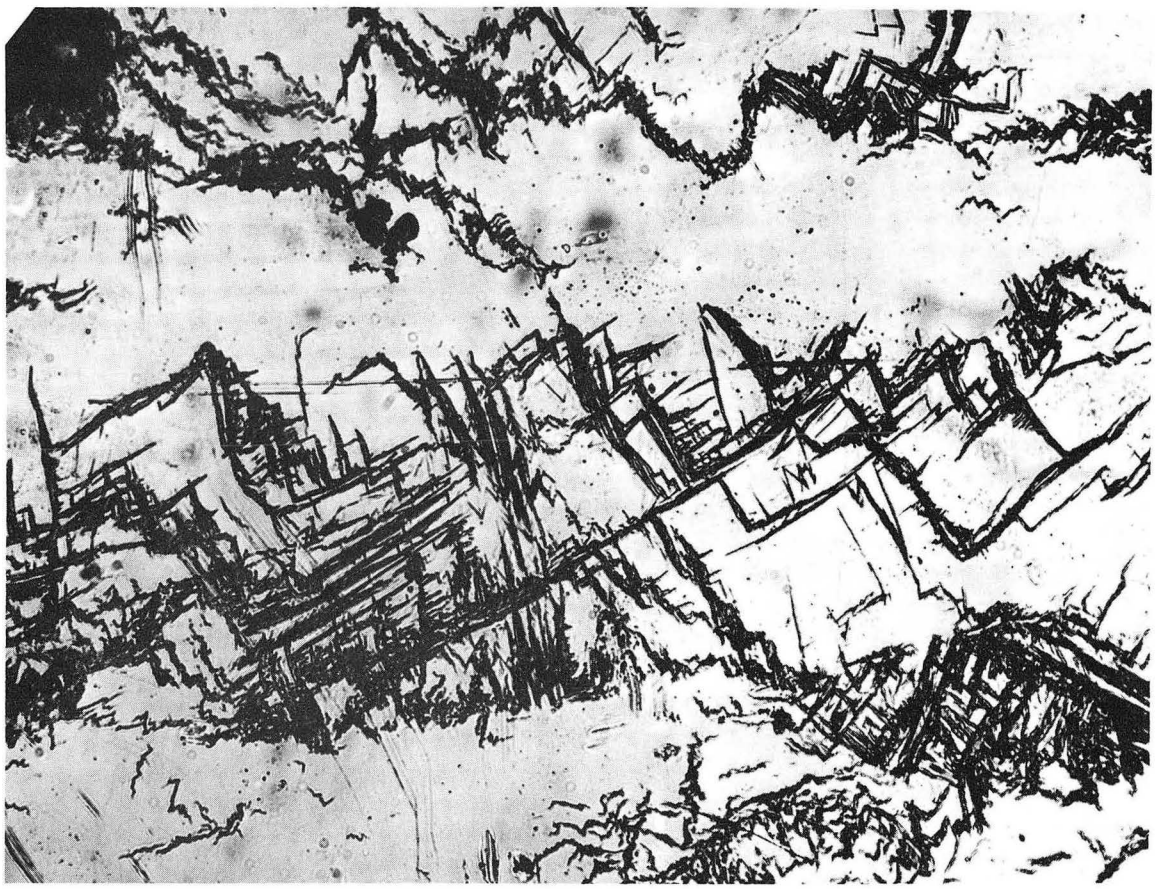

ZN-4952

Fig. 19

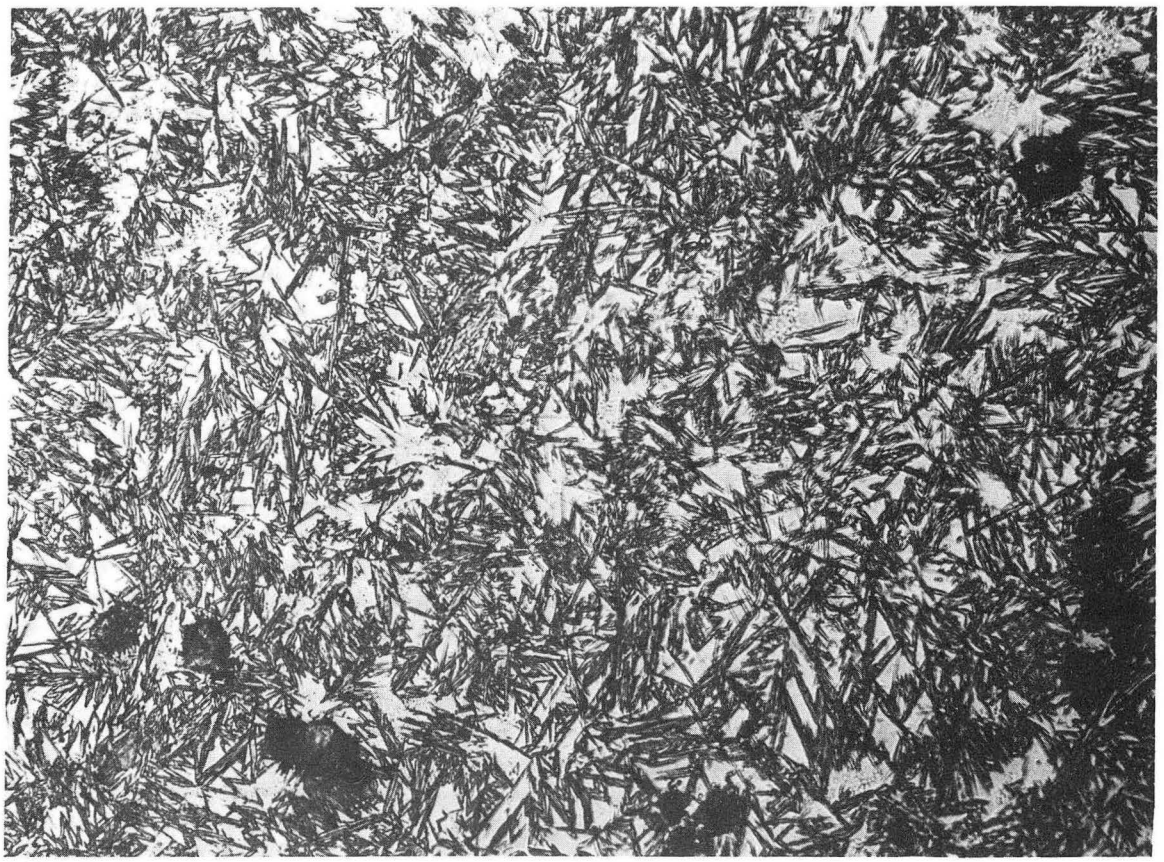

ZN-4946

Fig. 20

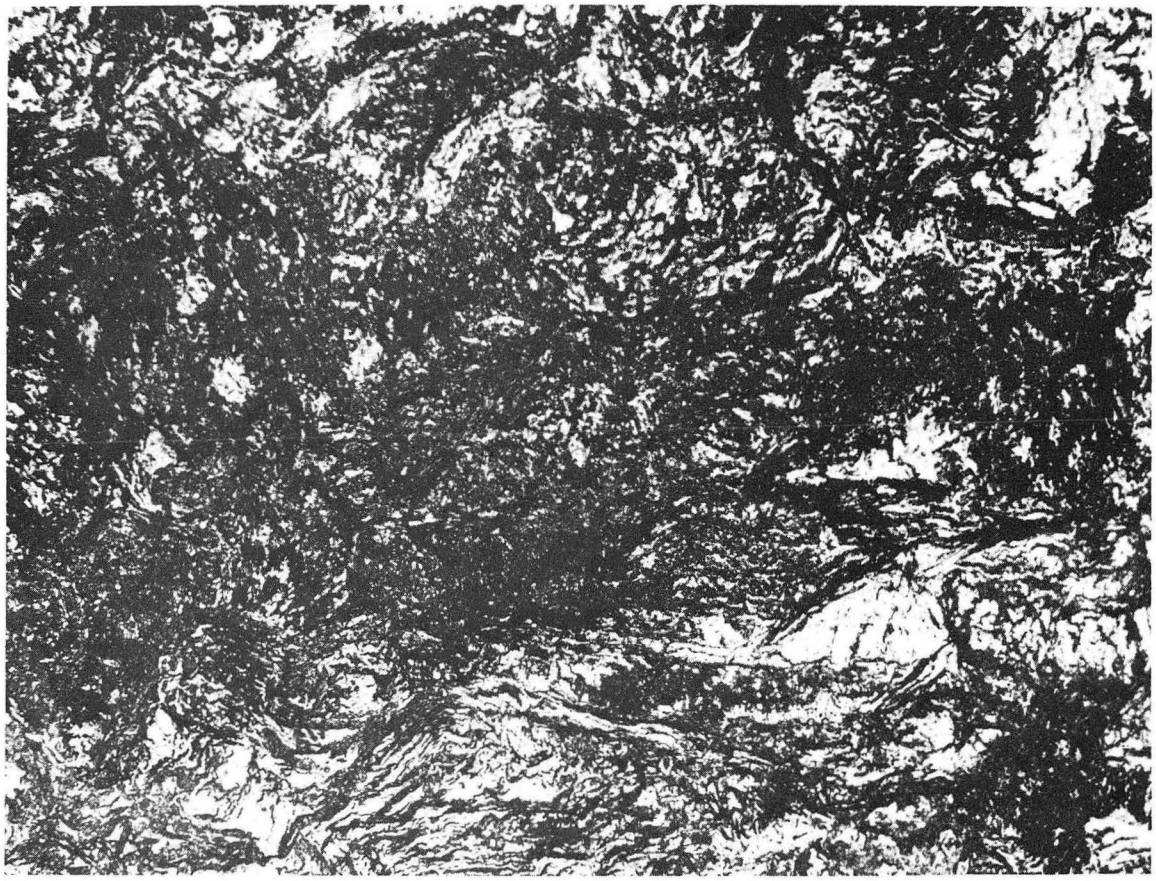

ZN-4941

Fig. 21

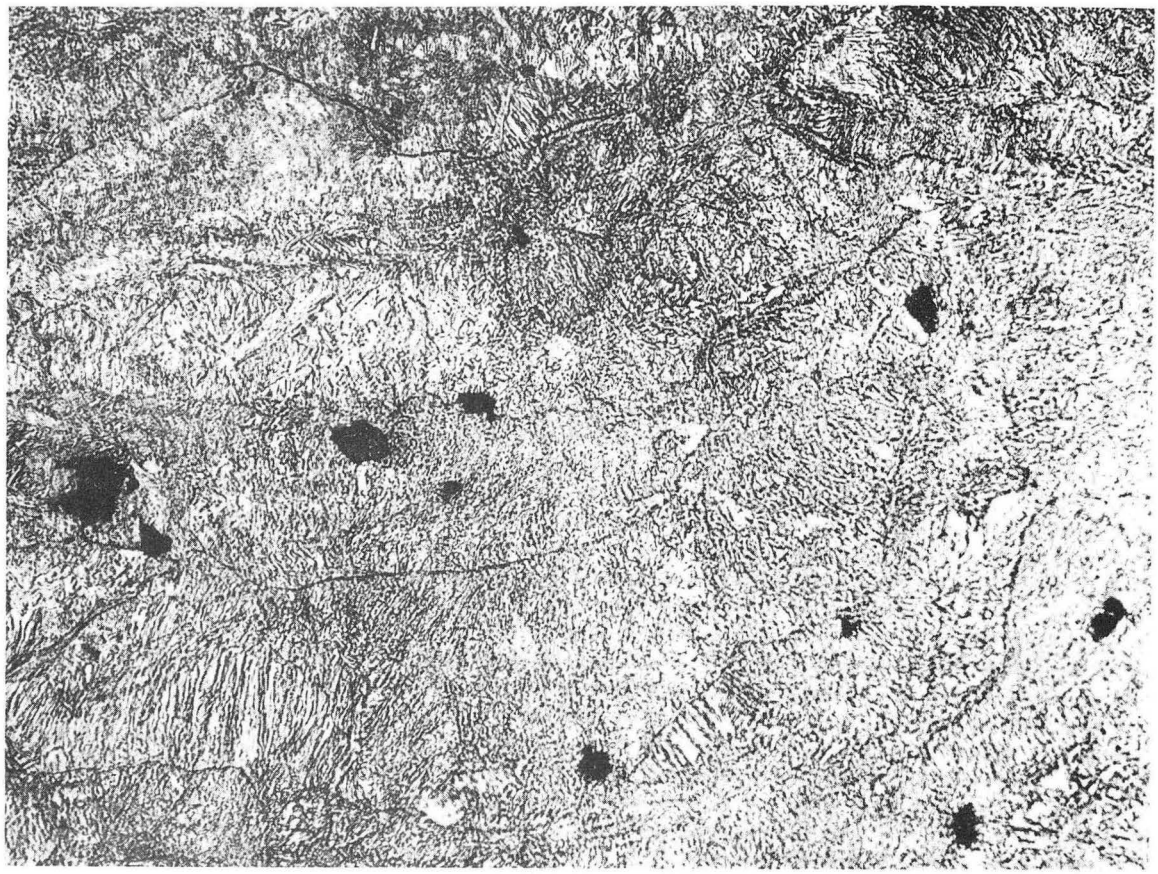

ZN-4948

Fig. 22

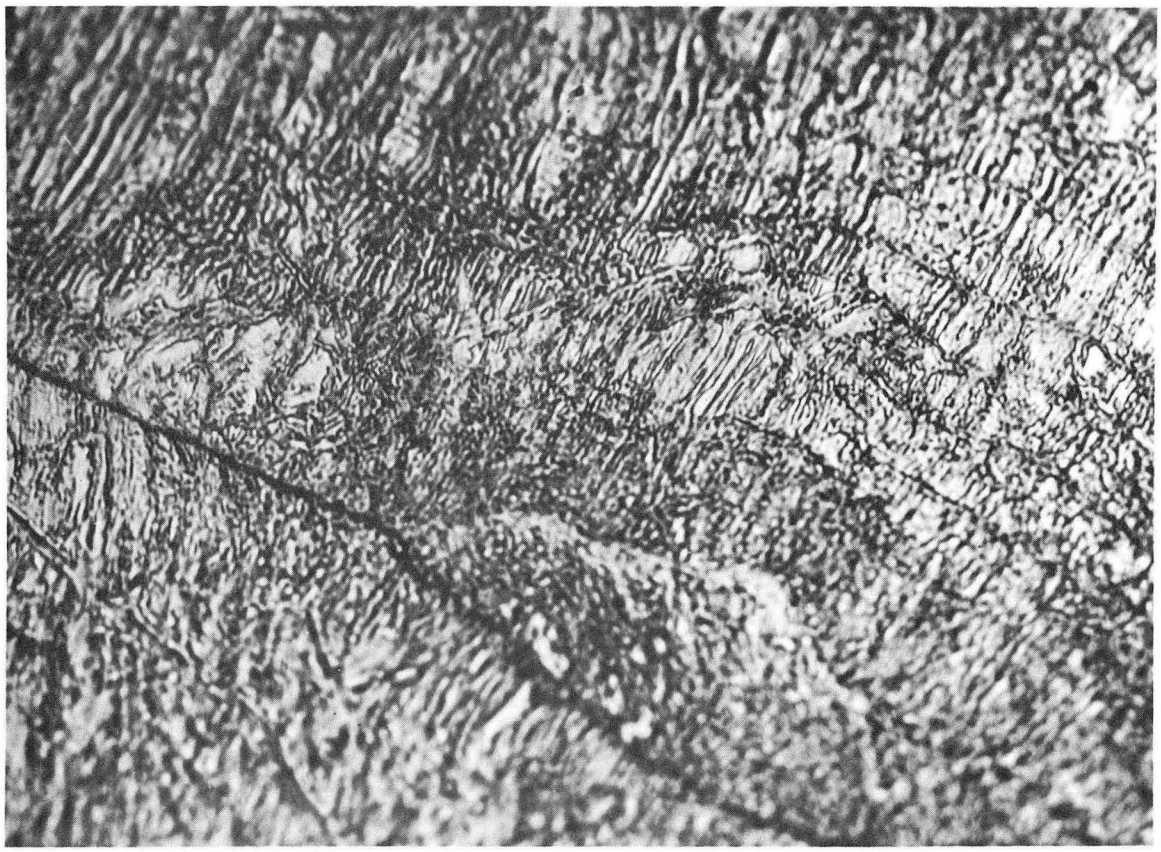

ZN-4947

Fig. 23

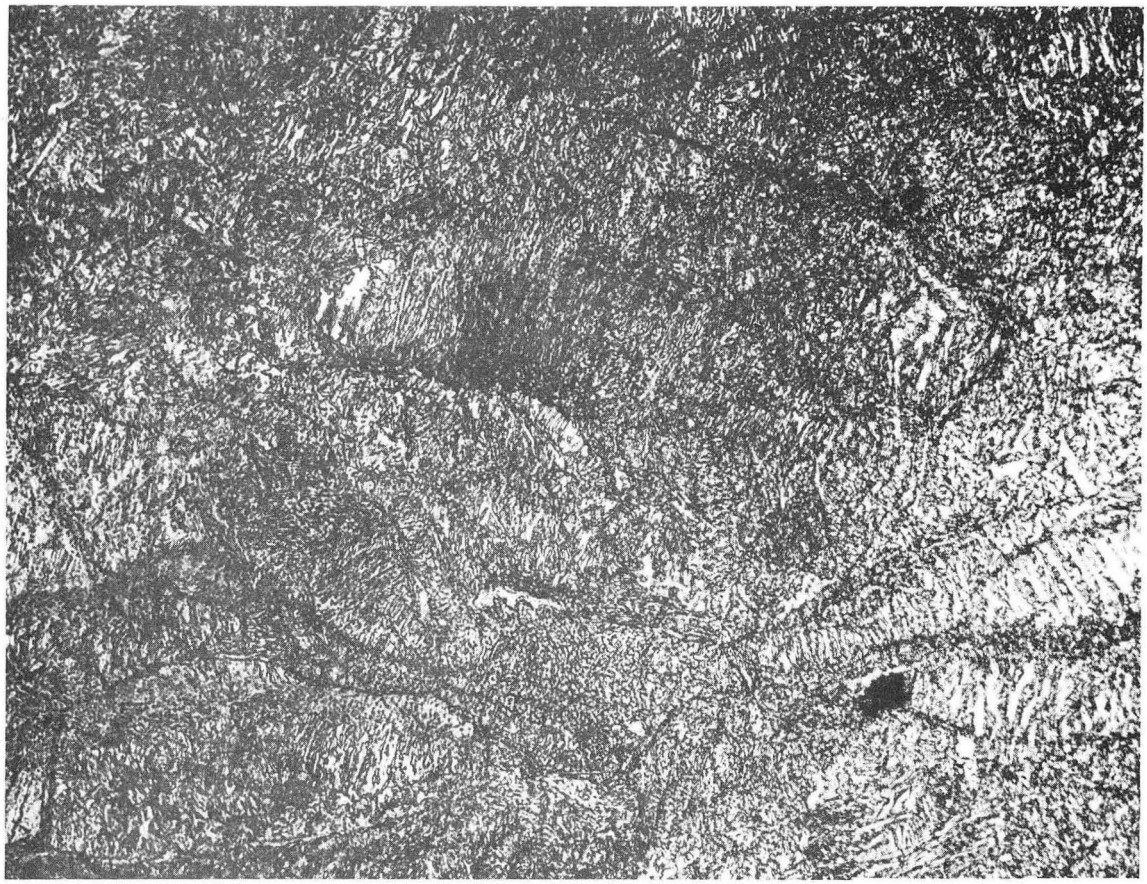

ZN-4949

Fig. 24

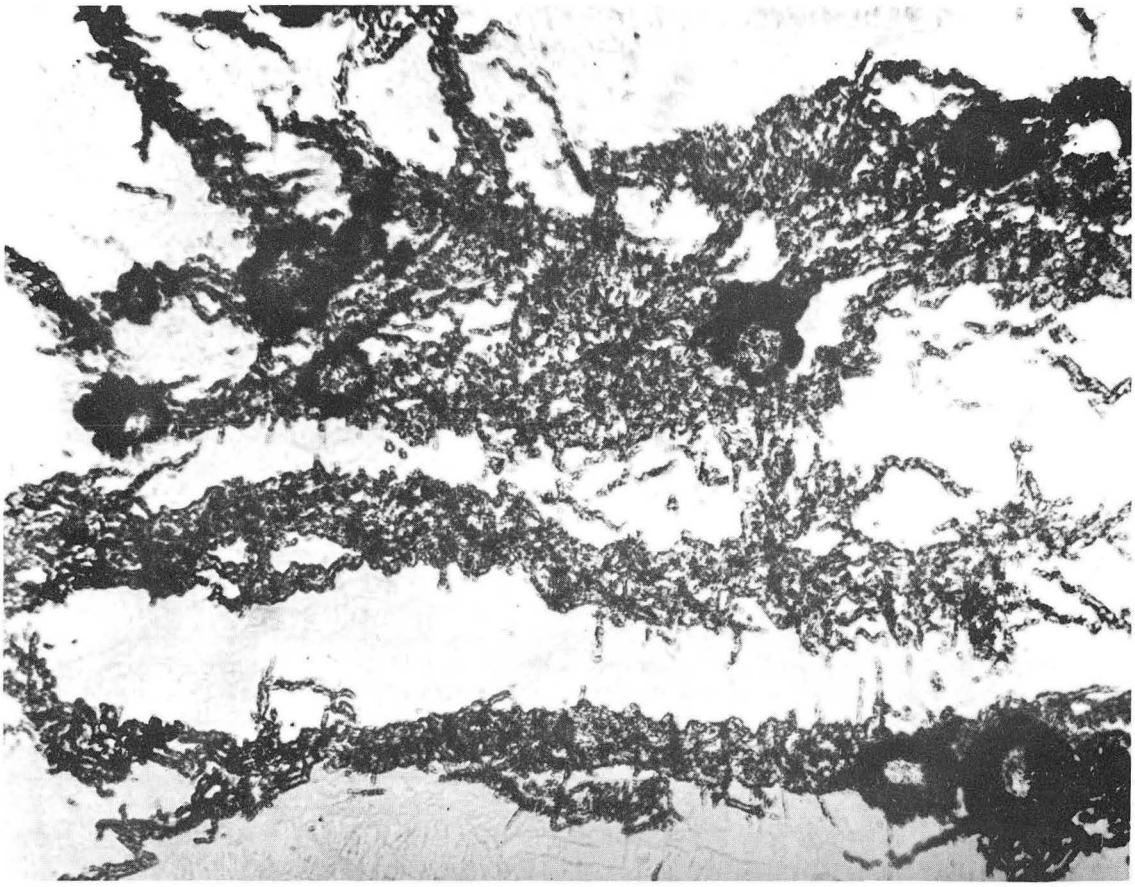

ZN-4954

Fig. 25

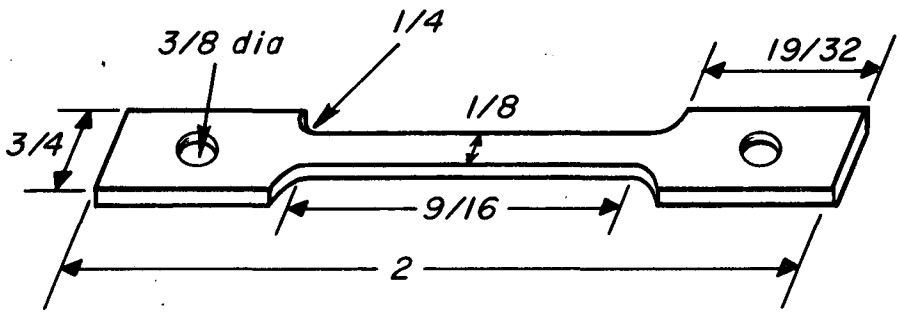

Measurements in inches
(not to scale)

Thickness - 1/8 max
Gage length - 0.5 ± 0.001

MU-35941

Appendix A